FLORIDA STATE UNIVERSITY

DEPARTMENT OF METEOROLOGY

TECHNICAL REPORT

The Distribution of Horizontal Divergence in a Topographically Perturbed Zonal Current

By Masamichi Oi

PREPARED UNDER PROJECT NR 082 071, CONTRACT NONR-988(01)

WITH THE OFFICE OF NAVAL RESEARCH

15 AUGUST 1954

THE DISTRIBUTION OF HORIZONTAL DIVERGENCE IN A TOPOGRAPHICALLY PERTURBED ZONAL CURRENT

By Masamichi Oi

This report has been prepared under Contract Nonr-988(01), Project NR 082 071, between the Office of Naval Research and Florida State University. Mr. Oi participated as a Graduate Assistant, while on leave from Osaka Gakugei University, where he is Assistant Professor of Meteorology and to which he has returned.

Werner A. Baum
Principal Investigator

Abstract

In this report the author deals with an extension of his previous work on the distribution of horizontal divergence of an incompressible flow around a semi-circular infinite cylinder with no upper boundary (Oi, 1952) to a more realistic case of flow over a semi-elliptic infinite cylinder with no upper boundary and to two cases of flow with upper boundaries. In terms of these results, the upstream trough is interpreted by the so-called vorticity equation.

1. Introduction

The deviations of zonal currents due to orographic effects have been treated by many authors, but it seems that almost all of them pay attention only to phenomena downstream from the obstacle and overlook upstream phenomena. Of course this procedure is practical when one is dealing with such a small-scale phenomenon as the Bishop-cloud, for there it seems possible to explain the phenomenon almost completely. However, it may be necessary to pay attention to upstream phenomena when one deals with large-scale bending of a westerly current on the scale of a cyclone perturbation.

Hitherto, it has been assumed that the inertial effect of a barrier does not reach upstream or downstream from the barrier (for example, V. Bjerknes et al, 1933, J. Holmboe et al, 1945, J. Charney and A. Elliassen, 1949, B. Bolin, 1950). However, this is too great a simplification of the phenomenon. As the author pointed out in his previous paper (Oi, 1952), in the case of a flow around a semi-circular infinite cylinder, we find a distribution of horizontal divergence as shown in fig. 1. As is evident from the lower picture, a vertical air column in the lower layer stretches at first in the upstream region and then shrinks near the barrier and vice versa in the downstream region. Thus we find convergence ahead of divergence upstream and divergence behind convergence downstream. Therefore, we can expect an upstream trough to be formed in addition to the downstream trough which earlier investigators have explained. For reference, the expres-

sion for the horizontal divergence is reproduced here:

$$\frac{\partial u}{\partial x} = 2 a^2 \frac{U \cos \chi_0}{r^3} \cos \theta (1 - 4 \sin^2 \theta),$$

where r, θ = polar coordinates, where the origin is the same as for the Cartesian coordinates, i.e., at the center of the circular cylinder, u = eastward velocity component, x = horizontal eastward Cartesian coordinate, a = radius of circular cylinder, U = uniform speed of flow at infinity, and χ_0 = the angle which the flow at infinity makes with the normal to the barrier. But, in this case, the distribution of the absolute value of $\frac{\partial u}{\partial x}$ shows that it is much larger over the upslope and downslope regions than upstream and downstream from the barrier, thus minimizing the upstream trough. Consequently, if this result holds for the more realistic case of a semi-elliptic cylinder, we shall have to consider the customary picture of nothing but horizontal divergence along the upslope region and horizontal convergence along the downslope region as reasonable and valid in practice.

2. <u>Incompressible two-dimensional flow over a semi-elliptic infinite cylinder with no upper boundary</u>

Parallel with the previous case, the fluid is assumed to be incompressible and ideal. The motion is assumed to be steady and irrotational in any vertical plane perpendicular to this elliptic cylinder; and at an infinite distance from the barrier both vertically and horizontally, the fluid moves horizontally with speed U m/sec at an angle χ_0 with the normal to the mountain axis. The kinematic boundary condition is assumed, so the fluid in contact with the elliptic barrier has no radial velocity in a vertical cross section.

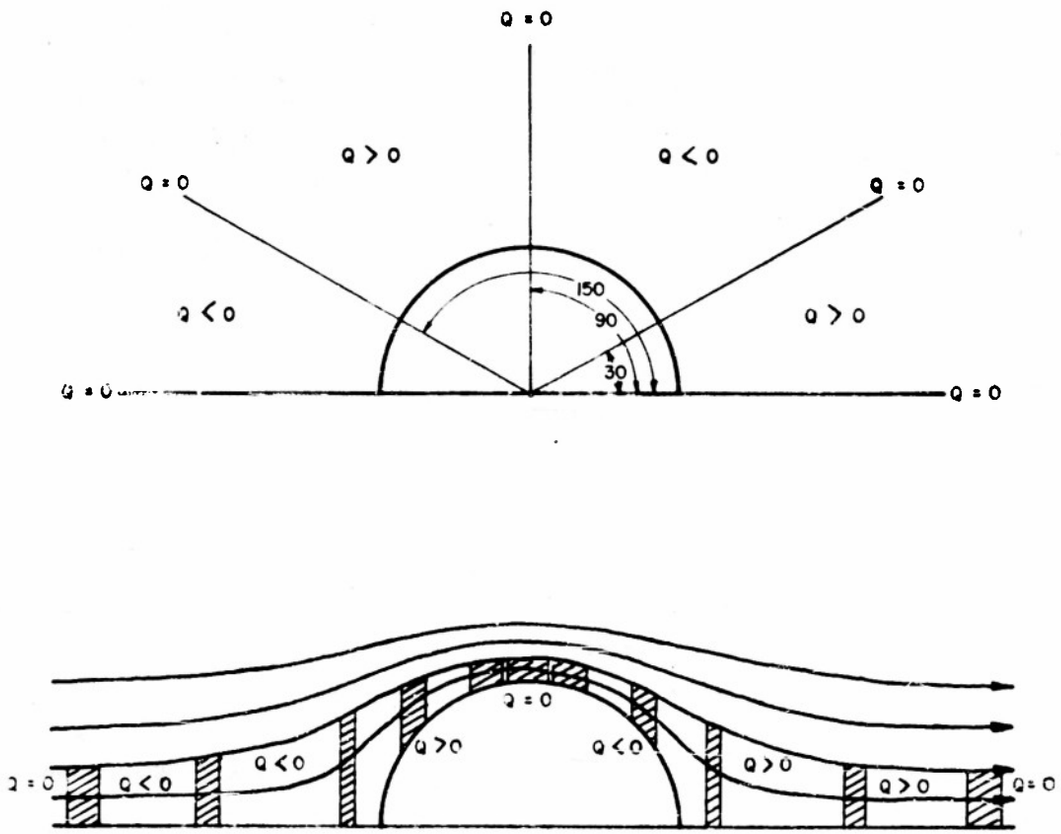

Fig. 1 Distribution of horizontal divergence of an ideal incompressible flow of infinite depth around a semi-circular infinite cylinder,
upper: numerically,
lower: illustratedly.
Here, $Q = \frac{\partial u}{\partial x}$ is the horizontal divergence.

In this case the velocity has a potential which is given as follows (for instance see Milne-Thompson, 1950):

$$\varpi = -U \cos \chi_0 \cdot (a + b) \cosh (\zeta' - \zeta_0'), \qquad (1)$$

$a^2 - b^2 = c^2$

$a = c \cosh \xi_0'$

$b = c \sinh \xi_0'$

$\zeta' = \xi' + i \eta'$

$x = c \cdot \cosh \xi' \cdot \cos \eta'$

$z = c \cdot \sinh \xi' \cdot \sin \eta'$

$Z = x + iz = c \cosh \zeta'$.

a = half length of major axis

b = half length of minor axis

$i^2 = -1$

Therefore, we can get easily

$$u = \frac{U \cos \chi_0 (a + b)}{c} \cosh \xi_0' - \frac{U \cos \chi_0 (a + b)}{2c} \cdot \sinh \xi_0' \frac{\sinh 2\xi'}{\sinh^2 \xi' + \sin^2 \eta'} \qquad (2)$$

$$w = - \frac{U \cos \chi_0 (a + b)}{2c} \sinh \xi_0' \cdot \frac{\sin 2\eta'}{\sinh^2 \xi' + \sin^2 \eta'} . \qquad (3)$$

Here ϖ = complex potential, U = magnitude of the velocity at infinity, u = horizontal velocity component normal to the barrier, positive eastward, and, w = vertical velocity component.

If we take the partial derivative of u with x, we have the horizontal divergence in this case:

$$\frac{\partial u}{\partial x} = \frac{\partial u}{\partial \xi'} \frac{\partial \xi'}{\partial x} + \frac{\partial u}{\partial \eta'} \frac{\partial \eta'}{\partial x}$$

$$= 2k \frac{\sinh \xi' \cdot \cosh^2 \xi' \cdot \cos^2 \eta'}{c(\sinh^2 \xi' + \sin^2 \eta')} (\tanh^2 \xi' - 3 \tan^2 \eta'). \qquad (4)$$

Here

$$k \equiv \frac{U \cos \chi_0 (a + b)}{c} .$$

From (4), we can easily find that $\frac{\partial u}{\partial x}$ becomes zero on the z-axis, i.e., along the vertical plane which goes through the summit of this barrier, and it becomes zero, also, along the curve which is

represented by

$$\tanh^2\xi' - 3\tan^2\eta' = 0.$$

This curve, as shown in fig. 2, is one branch of a rectangular hyperbola with the straight lines $\theta = 30°$ and $\theta = 150°$ as asymptotes in the first and second quadrants respectively. These are the lines of zero horizontal divergence.

To study the behavior of $\frac{\partial u}{\partial x}$, let us change variables from ξ', η' to Cartesian coordinates x, z,

$$\frac{\partial u}{\partial x} = \pm \frac{\sqrt{2}\, U \cos\chi_0 (a+b)\cdot b\left[3x^2z^2 - \frac{1}{4}\left[\sqrt{(c^2+z^2-x^2)^2+4x^2z^2} - (c^2+z^2-x^2)\right]\right]}{\sqrt{\sqrt{(c^2+z^2-x^2)^2+4x^2z^2} - (c^2+z^2-x^2)}\cdot\left[(c^2-x^2-z^2)^2 + 4c^2z^2\right]^{3/2}} \quad (5)$$

Here the plus and minus signs correspond to negative and positive values of x.

Using this expression, if we make an approximation for the practical case where we can consider $a \gg b$ (later we shall compute for the case where $a = 100b$), and moreover, if we consider $\frac{\partial u}{\partial x}$ far from the summit of the barrier so that $x \gg z$, we get

$$\frac{\partial u}{\partial x} \doteq \pm \frac{U\cos\chi_0 a\cdot b}{(x^2-d^2)^{3/2}}, \quad (6)$$

where $x \gg z$ and $a \gg b$, and $\pm$ correspond to the $\pm$ signs of x.

From (6), we know the horizontal divergence due to this orographical inertial effect is not only proportional to the cross-sectional area, but if the cross-sectional area is the same, a lower and wider barrier is more effective. Takahashi (1951) suggested that the dimension of the Eurasian continent is related to the wavelength of the westerlies. His idea is thus substantiated by this computation. And also, from this computation we can anticipate that in spite of the small difference of height

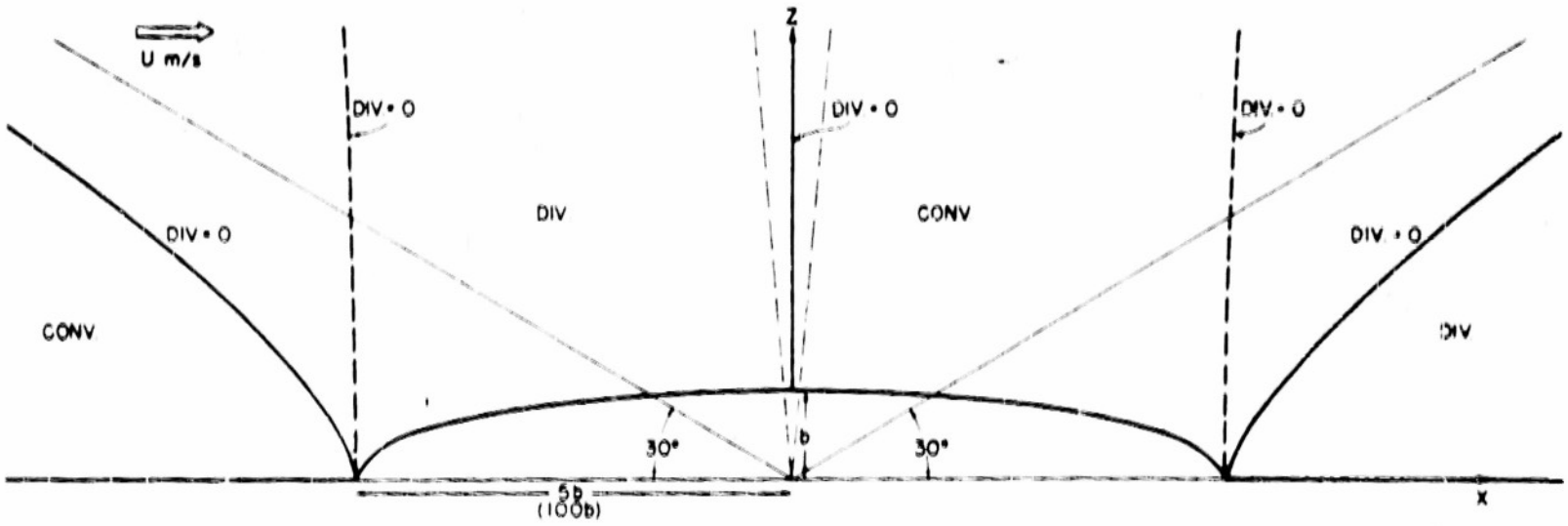

Fig. 2 Distribution of horizontal divergence of an ideal incompressible flow around a semi-elliptic infinite cylinder with no upper boundary for both cases, a = 5b, a = 100b; the former is expressed by thick lines, the latter by broken lines.

between the North American Rockies and South American Andes, the influence of the former mountain range upon the westerlies should be much greater than that of the latter.

To illustrate the distribution of $\frac{\partial u}{\partial x}$ given in (5), let us examine the case where $\chi_0 = 0$, U = 10 m/sec, a = 100 b, and b = 5 km. The results of the calculation are shown in fig. 3. Here the nondivergence line is almost vertical from the ground to a height of several times the barrier, and furthermore the absolute values of horizontal divergence are almost the same upstream and downstream from the barrier as immediately over the barrier. Thus we do have to take into consideration horizontal convergence and horizontal divergence upstream and downstream from the barrier as well as immediately over the upslope and downslope regions of the barrier. The previous result, for the case of a semi-circular cylindrical barrier, is a limiting case of the present one, for if, in expression (5), we put a = b we reduce to the previous result. As far as the qualitative distribution of horizontal divergence is concerned, there are no essential differences between the two cases; but quantitively we find that we must take into consideration upstream and downstream divergence even at a moderate distance from the foot of the obstacle.

Let us now consider what should be the effect of this distribution of horizontal divergence upon the bending of a zonal current. In the northern hemisphere, cyclonic rotation prevails upstream, but anticyclonic vorticity is gained gradually in the upslope and downslope regions. Cyclonic vorticity is developed

downstream. Thereafter the current gains anticyclonic vorticity and then undulates due to the meridional term of the vorticity equation. These results do not take into account the effect of the meridional convergence term in the horizontal divergence.

One further point should be made about the vertical deviation of flow due to the inertial effect of this semi-elliptic cylindrical barrier. In the case of a semi-circular cylindrical barrier, along the vertical through the summit the elevation of a streamline over its original height is given by (Oi, 1952)

$$h_{(z)} = \frac{a^2}{z},$$

where a = radius of circular cylinder (height of the barrier), and z = vertical component of Cartesian coordinates of a point on the vertical axis, i.e., height of this point. In the case of a semi-elliptic cylindrical barrier, this elevation is given by

$$h_{(z)} \doteqdot b - \frac{b}{a} z \quad . \tag{7}$$

If $b \ll a$, as it usually is, then $h_{(z)}$ does not change much with height. This is a very interesting result which means that the vertical influence reaches to very high levels. In actual situations this sometimes seems to be so, but at other times it does not. To portray the latter observed case, using an incompressible fluid, we have to consider a model in which the flow is confined between two horizontal parallel boundaries. Actually these two planes often correspond to the ground surface and the tropopause. Let us consider in the next section the cases of semi-circular cylindrical and semi-elliptic cylindrical barriers

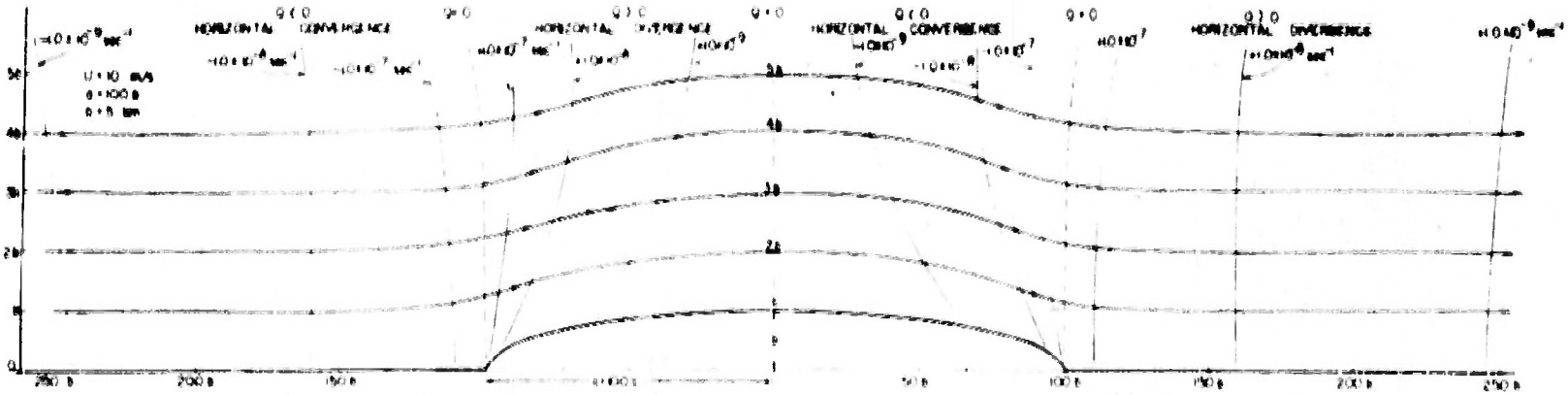

Fig. 3 Magnitude of horizontal divergence of an ideal incompressible flow around a semi-elliptic infinite cylinder (major axis (a) = 500 km, minor axis (b) = 5 km) with no upper boundary. Note the rapid transition from $Q < 0$ to $Q > 0$ over the foot of the barrier.

with upper boundaries.

3. Case of flow over a semi-circular infinite cylindrical barrier with a horizontal rigid upper boundary

As it is difficult to obtain a solution for the case of a perfect circular cylinder by ordinary treatments, we shall try to find an approximate solution by substituting an oval barrier which is very similar to a circular one. Superposing the flow caused by infinite series of doublets along the z-axis, and the general uniform flow, the speed of which is U m/sec parallel to the x-axis, we get an approximate solution for this case. Referring to any hydrodynamical text book (i.e., Streeter, 1948), we can get the complex potential for this case:

$$\varpi = \phi + i\psi$$

$$= -UZ + C' \coth \frac{\pi Z}{d} \ , \ Z = x + iz \ , \qquad (8)$$

where C' is a constant to be decided by boundary conditions and d is the distance between two adjacent doublets. Therefore, if we take h as the height of an upper boundary, i.e., d = 2h, then C' can be determined easily by setting the value of the stream function which represents the lower boundary equal to zero. Let us consider a couple of examples. At first if h is twice the height of barrier,

$$\psi = -Uz - C' \frac{\sin \frac{\pi z}{h}}{\cosh \frac{\pi x}{h} - \cos \frac{\pi z}{h}} = 0 \ .$$

$$\therefore \quad Uz \left(\cos \frac{\pi z}{h} - \cosh \frac{\pi x}{h} \right) = C' \sin \frac{\pi z}{h} \ .$$

Let $x \to 0$, $z \to \frac{h}{2}$,

then $U\frac{h}{2}\left(\cos\frac{\pi}{2} - 1\right) = C'\sin\frac{\pi}{2}$,

$$C' = -\frac{Uh}{2} .$$

On the other hand,

$$z \to 0,\ x \to \pm\, a\left(= \frac{h}{2}\right) .$$

$$\therefore\ 1 - \cosh\frac{\pi}{2} = \frac{C'}{U}\frac{\pi}{h} ,\ C' = -\frac{Uh}{2}\,\frac{1.508}{\frac{\pi}{2}} ,$$

$$C' \doteqdot -\frac{Uh}{2}$$

within 2-3% error. Then putting $C' = -\frac{Uh}{2}$, we can take both axes approximately equal, and we can consider this stream line $\psi = 0$ as one which represents the ground boundary surface in the case of the semi-circular cylindrical barrier. And also for the case where the height of the barrier is 1/5 of the height of upper boundary, we can easily find

$$C' \doteqdot -\frac{Uh}{5\pi} .$$

Turning back to the main subject, we get

$$u = -\frac{\partial\phi}{\partial x} = U + C'\frac{d}{dx}\left[\frac{\sinh\frac{\pi}{h}x}{\cosh\frac{\pi}{h}x - \cos\frac{\pi}{h}z}\right]$$

$$= U - C'\frac{\pi}{h}\,\frac{1 - \cosh\frac{\pi}{h}x\cdot\cos\frac{\pi}{h}z}{\left(\cosh\frac{\pi}{h}x - \cos\frac{\pi}{h}z\right)^2} .$$

Therefore, we get finally

$$\frac{\partial u}{\partial x} = C'\left(\frac{\pi}{h}\right)^2\frac{\sinh\frac{\pi}{h}x\left[2 - \cos^2\frac{\pi}{h}z - \cos\frac{\pi}{h}z\cdot\cosh\frac{\pi}{h}x\right]}{\left(\cosh\frac{\pi}{h}x - \cos\frac{\pi}{h}z\right)^3} \qquad (9) .$$

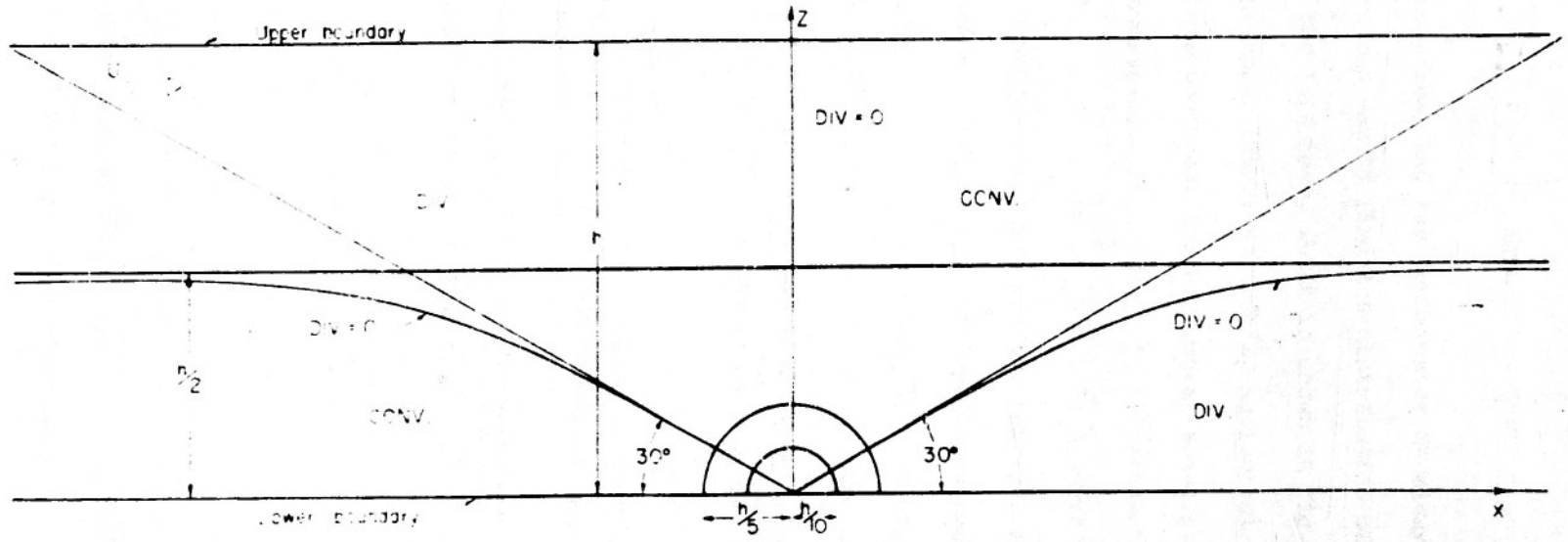

Fig. 4 Distribution of horizontal divergence of an ideal incompressible flow with an upper boundary around a semi-circular infinite cylinder for cases where the radii are equal to h/5 and h/10, h is the height of the upper boundary.

In (9), C' is always negative, and the denominator is always positive. From (9), we can easily find the distribution of horizontal divergence for this case, which is shown in fig. 4. Here we see that in the upper layer, above h/2, horizontal divergence prevails everywhere upstream, and horizontal convergence prevails everywhere downstream. This result is independent of the height of the barrier. The curve of $\frac{\partial u}{\partial x} = 0$ is a curve which has two asymptotes as x approaches $\pm\infty$, and two tangents at x = 0, i.e., the horizontal straight line through the origin, which are the lines of $\frac{\partial u}{\partial x} = 0$ for the same case with no upper boundary ($\theta = 30°$ and $150°$). This curve is not affected by the height of the barrier and is determined only by the height of the upper boundary. Furthermore, except at $z \doteqdot h/2$, its shape is very nearly that of the straight lines: $\theta = 30°$ or $\theta = 150°$. Below these curves, on the upstream side, horizontal convergence prevails, and on the downstream side, horizontal divergence prevails. Therefore in the lower half layer the distribution of horizontal divergence is very similar to the case with no upper boundary.

Next, let us examine the differences which exist between the cases with no upper boundary and with an upper boundary for the same geometrical point.

As can be seen in table 1, in the convergence domain of the lower layer on the upstream side at points far from the foot of the barrier, the value of the horizontal divergence is rather smaller and, on the other hand, at points near the foot of the

Table 1

Comparison of values of horizontal divergence in the case with no upper boundary and in the case with an upper boundary whose height is twice as large as the radius of the semi-circular cylinder.

Position of points	Case	No upper boundary	Upper boundary at $z = h$
x	z	$\frac{U}{h}$ (sec^{-1})	$\frac{U}{h}$ (sec^{-1})
$-\frac{5}{4}h$	$\frac{h}{4}$	- 0.20	- 0.14
$-h$	$\frac{h}{4}$	- 0.34	- 0.30
$-\frac{7}{8}h$	$\frac{h}{4}$	- 0.445	- 0.36
$-\frac{13}{16}h$	$\frac{h}{4}$	- 0.51	- 0.51
$-\frac{3}{4}h$	$\frac{h}{4}$	- 0.58	- 0.59
$-\frac{1}{2}h$	$\frac{h}{4}$	- 0.51	-31.5
$-h$	$\frac{h}{2}$	- 0.02	+ 0.08
$-\frac{h}{2}$	$\frac{h}{2}$	+ 1.00	+ 1.44
$-h$	$\frac{3}{4}h$	+ 0.09	+ 0.30
$-\frac{h}{2}$	$\frac{3}{4}h$	+ 0.12	+ 1.12

barrier, it is much larger than in the case of no upper boundary. This is especially notable when the height of the barrier is rather large compared with the height of the upper boundary (in this case, h/2), and less notable if the height of barrier is rather small compared with the height of the upper boundary (say 1/5h). In the divergence domain of the upper layer, the magnitude of horizontal divergence behaves similarly but not so strongly as in the convergence domain. The downstream results may be obtained in a similar fashion.

4. Case of flow over semi-elliptic infinite cylindrical barrier with horizontal rigid upper boundary

If the semi-circular cylinder is a perfect one and has no upper boundary, we can theoretically apply the so-called Joukowski transformation to velocity potential. This transformation will deform the semi-circular cylinder in the vertical plane to a semi-elliptic cylinder. However, in the previous treatment, the barrier is not exactly a circular cylinder and, moreover, we have an upper boundary. Therefore we can not apply this transformation. Thus, the author has adopted a new method to get the velocity potential for this case. He considered infinite series of equally spaced sources and sinks of equal strength, distributed along two straight lines parallel to the z-axis, and superposed two velocity potentials for this set of infinite series and for uniform flow parallel to the x-axis.

The complex potential for a flow caused by an infinite series of sources of strength $2\pi C$ at equal distances d(= 2h, h is the height of the upper boundary), as given by Streeter (1949), is

$$\omega = - C \ln \sinh \frac{\pi Z}{d} , \qquad (10)$$

where $Z = x + iz$. Therefore, we get in a similar fashion the complex potential for such an infinite series of sources along an axis parallel to the z-axis at $x = - a$

$$\omega_1 = -C \ln \sinh \frac{\pi (Z + a)}{d} , \qquad (11)$$

where $d = 2h$. And likewise, for the complex potential for an infinite series of sinks of equal strength $- 2\pi C$ with an equal spacing, d, along an axis parallel to the z axis at $x = a$, we get

$$\omega_2 = C \ln \sinh \frac{\pi (Z - a)}{d} , \qquad (12)$$

where $d = 2h$.

The complex potential for a uniform flow with U m/sec toward the positive x direction is given by

$$\omega_3 = - UZ . \qquad (13)$$

Therefore, the complex potential for our purpose can be found by adding (11), (12) and (13). If we denote this by ω_t, then

$$\begin{aligned} \omega_t &= \omega_1 + \omega_2 + \omega_3 \\ &= - UZ - C \ln \left[\frac{\sinh \frac{\pi (Z + a)}{h}}{\sinh \frac{\pi (Z - a)}{h}} \right] \qquad (14) \\ &= \phi + i \psi . \end{aligned}$$

Here, a is approximately equal to the focal distance of this ellipse. If the ratio of the two axes is 100, a is equal to the focal distance within a 1% error. From (14) we can easily get,

$$\phi = - Ux - \frac{C}{2} \ln \left[\frac{\sinh \frac{\pi}{h} (x + a) - \cos \frac{\pi}{h} z}{\cosh \frac{\pi}{h} (x - a) - \cos \frac{\pi}{h} z} \right] , \qquad (15)$$

$$\psi = - Uz - C\left[-2\pi + \tan^{-1}\frac{\tan\frac{\pi z}{2h}}{\tanh\frac{\pi(x+a)}{2h}} - \tan^{-1}\frac{\tan\frac{\pi z}{2h}}{\tanh\frac{\pi(x-a)}{2h}}\right]. \quad (16)$$

Thus, we get

$$u = -\frac{\partial\phi}{\partial x} = U + \frac{C\pi}{h}\sinh\frac{\pi a}{h}\left[\frac{\cosh\frac{\pi a}{h} - \cosh\frac{\pi x}{h}\cos\frac{\pi z}{h}}{\left(\cosh\frac{\pi(x+a)}{h} - \cos\frac{\pi z}{h}\right)\left(\cosh\frac{\pi(x-a)}{h} - \cos\frac{\pi z}{h}\right)}\right]$$

and

$$\frac{\partial u}{\partial x} = -C\left(\frac{\pi}{h}\right)^2\sinh\frac{\pi a}{h}\sin\frac{\pi x}{h}\left[\frac{2\cosh\frac{\pi a}{h}\cosh\frac{\pi x}{h}\left(\cosh^2\frac{\pi a}{h} + \cosh^2\frac{\pi x}{h} + \sin^2\frac{\pi z}{h}\right)\cos\frac{\pi z}{h}}{\left(\cosh\frac{\pi(x+a)}{h} - \cos\frac{\pi z}{h}\right)^2\left(\cosh\frac{\pi(x-a)}{h} - \cos\frac{\pi z}{h}\right)^2}\right]. \quad (17)$$

From (17), we see that again $\frac{\partial u}{\partial x} = 0$ along the z axis, and the curves of $\frac{\partial u}{\partial x} = 0$ also have as asymptotes the horizontal line, $z = h/2$, and the curves of $\frac{\partial u}{\partial x} = 0$ pass through the points $x = \pm a$.

Let us now consider the values of C and a. For the case of $a = 100b$, $b = h/2$ we get, for the stream function,

$$\psi = - Uz - C\left[-2\pi + \tan^{-1}\frac{\tan\frac{\pi}{2}\frac{z}{h}}{\tanh\frac{\pi}{2}\frac{(x+a)}{h}} - \tan^{-1}\frac{\tan\frac{\pi}{2}\frac{z}{h}}{\tanh\frac{\pi}{2}\frac{x-a}{h}}\right].$$

On the stream line $\psi = 0$, at $x = 0$, $z = h/2$,

$$\therefore \frac{hU}{2} = -C\left[-2\pi + \tan^{-1}\frac{\tan\frac{\pi}{4}}{\tanh\frac{\pi a}{2h}} - \tan^{-1}\frac{\tan\frac{\pi}{4}}{\tanh\left(-\frac{\pi a}{2h}\right)}\right],$$

$$\frac{U}{C} = \frac{4}{h}\left[\pi - \tan^{-1}\frac{1}{\tan\frac{\pi a}{2h}}\right]. \quad (18)$$

At the stagnation point

$$\frac{d\omega}{dZ} = -U + \frac{C\pi}{h}\frac{\sinh\frac{\pi a}{h}}{\cosh\frac{\pi}{h}z - \cosh\frac{\pi a}{h}},$$

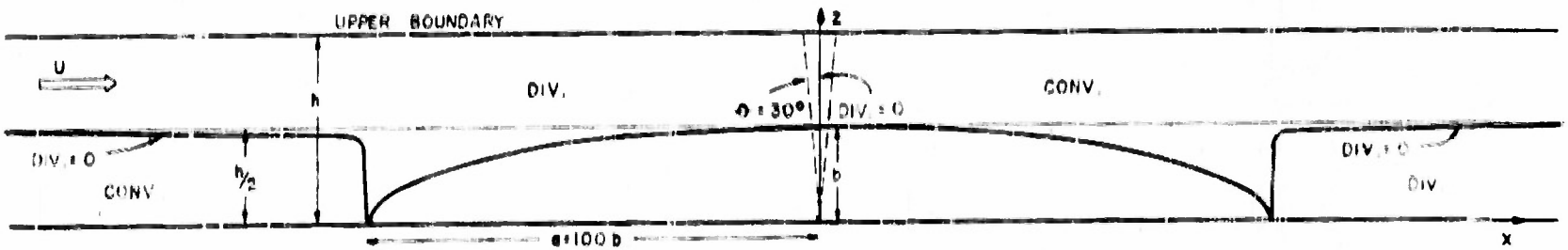

Fig. 5 Distribution of horizontal divergence of an ideal incompressible flow with an upper boundary around a semi-elliptic infinite cylinder for a case in which b = h/2 and a = 100b, where a is the length of major axis and b is the length of minor axis. h is the height of the upper boundary.

i.e.,

at $z = 0$, $x = \pm a$, $Z = \pm a$,

$$\frac{d\varpi}{dZ} = 0 \quad \therefore \quad \frac{U}{C} = \frac{\pi}{h} \frac{\sinh \frac{\pi a}{h}}{\cosh \frac{\pi}{h}(50h) - \cosh \frac{\pi a}{2h}} \qquad (19)$$

From (18) and (19)

$$\frac{\pi}{h} \frac{\sinh \frac{\pi a}{h}}{\cosh 50\pi - \cosh \frac{\pi a}{h}} = \frac{4}{h}\left[-\pi + \tan^{-1} \frac{1}{\tanh \frac{\pi a}{2h}}\right] .$$

$$\therefore \quad \tan \frac{\pi}{h} \frac{\sinh \frac{\pi a}{h}}{\cosh 50\pi - \cosh \frac{\pi a}{h}} = \frac{1}{\tanh \frac{\pi a}{2h}} .$$

Solving this numerically, we get $a \doteq 49.75\ h$ and $C = \frac{Uh}{\pi}$. For different values of b, say $b = 1/5h$, a does not change much. These results are shown in fig. 5 for the case of $b = h/2$.

As we saw in sections 3 and 4, in the case of flow with an upper boundary, horizontal divergence prevails everywhere upstream and horizontal convergence everywhere downstream above h/2, independent of the height of the barrier. On the other hand, in the lower half layer, as in the cases without an upper boundary, a horizontal convergence domain precedes the horizontal divergence domain both upstream and downstream. Therefore, from this result we can conclude there should be a nondivergence level in the atmosphere when the tropopause is strong enough to suppress the vertical motion. This level of nondivergence should be at about the half-effective height ($\frac{1}{2} H_e = \frac{1}{2} \frac{\int_0^h \rho \cdot g dz}{\rho g} \doteq \frac{1}{2} \frac{\int_0^h \rho dz}{\rho}$; i.e., 500mb). Upstream, above this nondivergence level ther exists horizontal divergence, with convergence below; while downstream, above this level there exists horizontal convergence, with diver-

gence below. A distribution of this sort was analyzed recently by H. Landers in his work downstream of the North American Rockies (unpublished). To aid interpretation, the coordinates of 10 points on this curve of nondivergence are tabulated in table 2.

As it is evident from this table, the curve $\frac{\partial u}{\partial x} = 0$ is almost vertical from the ground to nearly the height h/2 and then turns to the left and right, upstream and downstream, asymptotically to z = h/2. Hence, this nondivergence level can be considered almost horizontal upstream and downstream from the barrier, and almost vertical near the foot of the barrier.

Table 2

Coordinates of 10 points on the curve $\frac{\partial u}{\partial x} = 0$ for the case of an upper boundary, as multiples of h.

z	$\frac{1}{20}$	$\frac{2}{20}$	$\frac{3}{20}$	$\frac{4}{20}$	$\frac{5}{20}$	$\frac{6}{20}$	$\frac{7}{20}$	$\frac{8}{20}$	$\frac{9}{20}$	$\frac{10-1}{20\ 2}$
x	±49.83	±49.88	±49.92	±49.98	±50.04	±50.12	±50.22	±50.36	±50.65	± ∞

Here, the minor axis (b) = h/2, and major axis (a) = 50h.

This characteristic of zonal flow with an upper boundary can be seen in certain isentropic analyses in vertical cross-sections of actual zonal flows. For instance, the analyses by Hess and Wagner (1948) of waves over the northwestern United States, near the tropopause and also from 17,000 to 20,000 ft, showed neutral layers in which the flow was nearly horizontal. In their cross-sections (fig. 6), we can clearly see that not only the tropopause but also the layer from above 17,000 to 20,000 ft remain nearly undisturbed, descending motion occuring in the

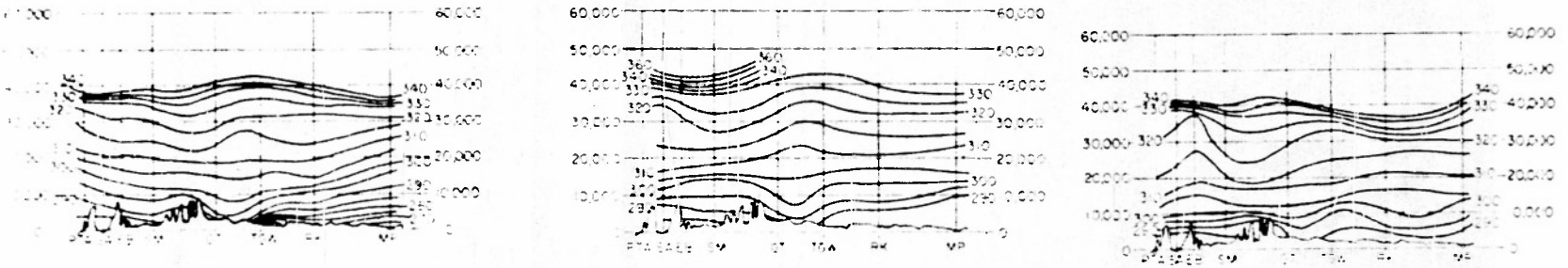

Fig. 6 Lines of constant potential temperature drawn across the western mountain mass of the United States from Tatoosh Island (PTA) through Seattle (SA), Ellensburg (EB), Spokane (SM), Great Falls (GT), Glasgow (TRW), Bismarck (BK) and Minneapolis (MP) for 1500Z 10, 0300Z 11 and 1500Z 11 January 1945, in which the vertical scale is in units of pressure-altitude (feet) of the U.S. standard atmosphere.

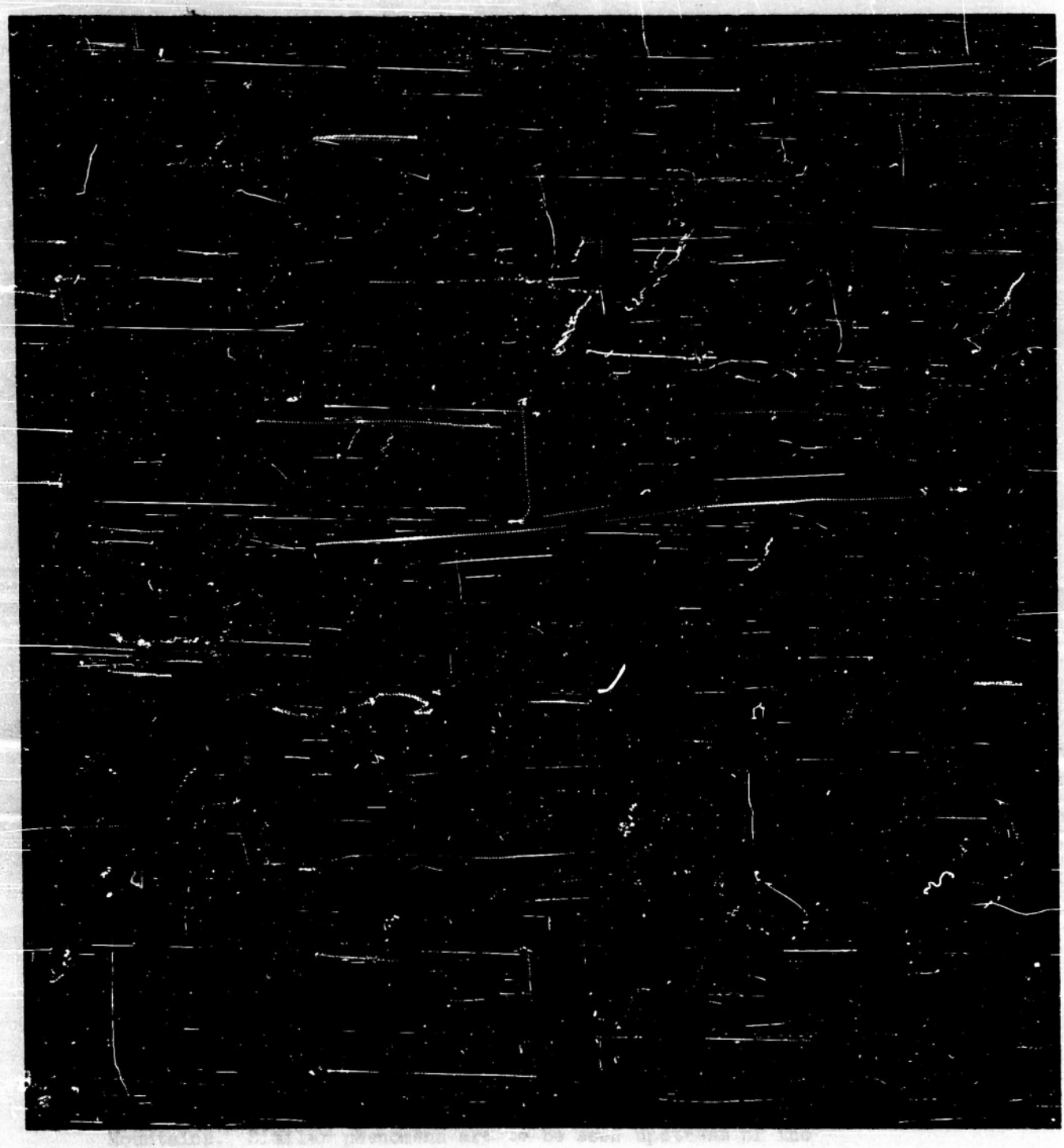

Fig. 7 Westerly flow crossing a pole-to-equator obstacle whose thickness is half of the depth of fluid shell.
The ratio of the relative angular velocity of the west wind to the absolute angular velocity of the west wind is 0.13.

lee beneath the nodal surface and ascending motion between this surface and the tropopause. There is a double structure of flow under the tropopause which coincides with the distribution of horizontal divergence in fig. 4.

In addition, Long and Fultz (Long 1952) carried out experiments with a rotating spherical fluid shell designed to produce orographical perturbations of a zonal current. In this experiment they have produced such a flow with an upper boundary crossing a barrier 90° of latitude long and about 10° longitude wide (fig. 7).

In this case (fig. 7), we can see not only the downstream trough and its train of undulations but also the upstream trough and in higher latitudes even closed perturbations. There is also some indication near the upstream trough of two kinds of trajectories at the same place. The main indication is the cyclonic curvature of the trough, but there are also signs of anticyclonic motions which are presumably at a higher elevation.

5. Further synoptic interpretations

There is a great deal of synoptic evidence which suggests the existence of horizontal convergence upstream from mountain chains.

Thus, the mean monthly 700 mb charts published in the Monthly Weather Review often show cyclonic curvature west of the Rocky Mountains. Similar phenomena are to be seen upstream of the coastal ranges of Europe and upstream of the Central Asian and Siberian mountain ranges (fig. 8).

Such upstream troughs can be seen also in ocean currents,

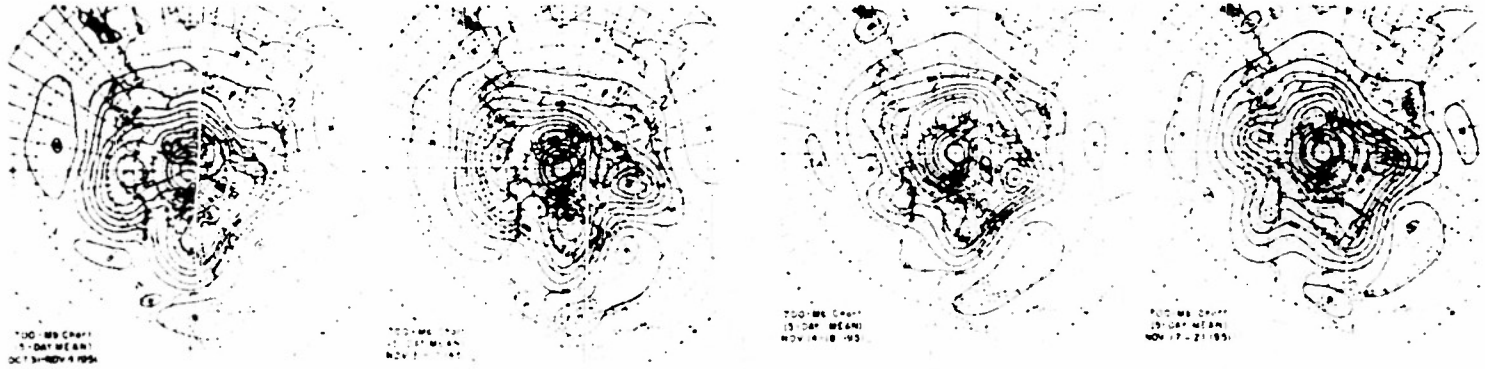

Fig. 8 Five days mean 700 mb charts for periods Oct. 31-Nov. 4, Nov. 5-Nov. 7, Nov. 14-18 and Nov. 17-21, 1951.

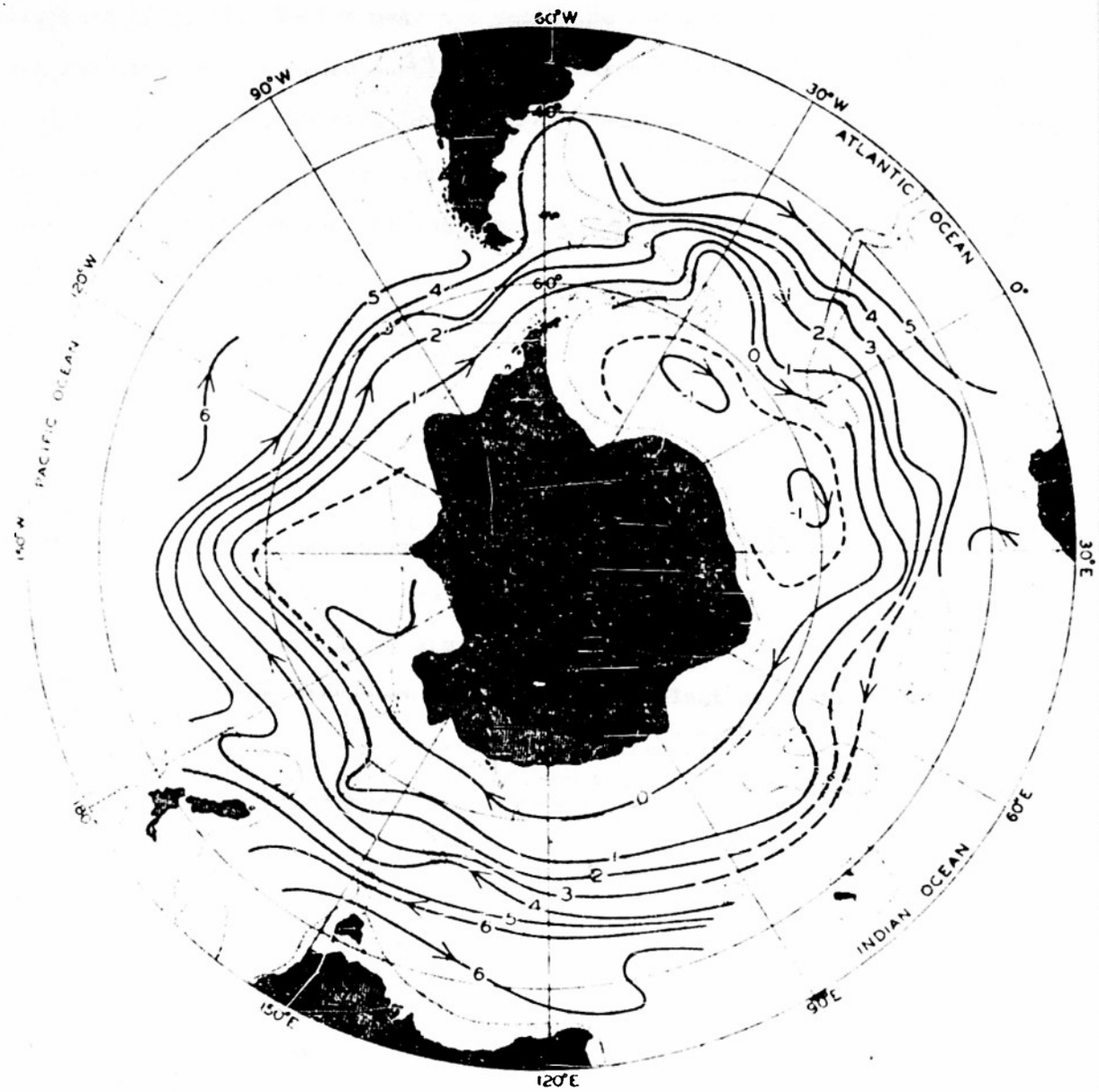

Fig. 9 Transport lines around the Antarctic Continent. Between two lines, the transport relative to the 3000-decibar surface is about 20 million cubic meters per second.

for example, in the mean oceanic transport lines of the southern hemisphere (fig. 9). We see near the submarine ridge in the South Atlantic Ocean (shaded part) that the current turns to the right on the upstream side, due to the horizontal convergence, although it should turn to the left according to the former customary explanation. We can see the same feature upstream of the submarine ridge in the South Indian Ocean. Thus, experimentally and synoptically, the actual features of a zonal current upstream from an orographical barrier seem to support the theory presented here.

As is self evident, this interpretation can be applied to the case of an aero-topographical barrier, such as a cold air dome or cold air mass against a warm air mass along a frontal zone, or even two air masses of similar characteristics encountering each other from different directions. This last case can be seen along the so-called equatorial front. Therefore, through this approach, we can interpret, in a somewhat different way from the usual one, the so-called wave theory of cyclones, as well as the formation of tropical cyclones in easterly zonal currents. Here, as an example of the effect of aero-topographical barriers, the work of Elliot (1951) is shown in fig. 10.

In this figure, we notice that the upstream trough, on the west side of the cold air outbreak, changes its position corresponding to the change of the position of the cold air outbreak.

Many meteorological dynamical or synoptic phenomena can be interpreted in this way; however, the author will discuss these

problems in later papers.

Acknowledgement: The author wishes to express his thanks to Professor W. Baum and the staff of the Florida State University, Department of Meteorology, for their support during his stay at that institution and he acknowledges also the help of Dr. S. Hess in editing this report.

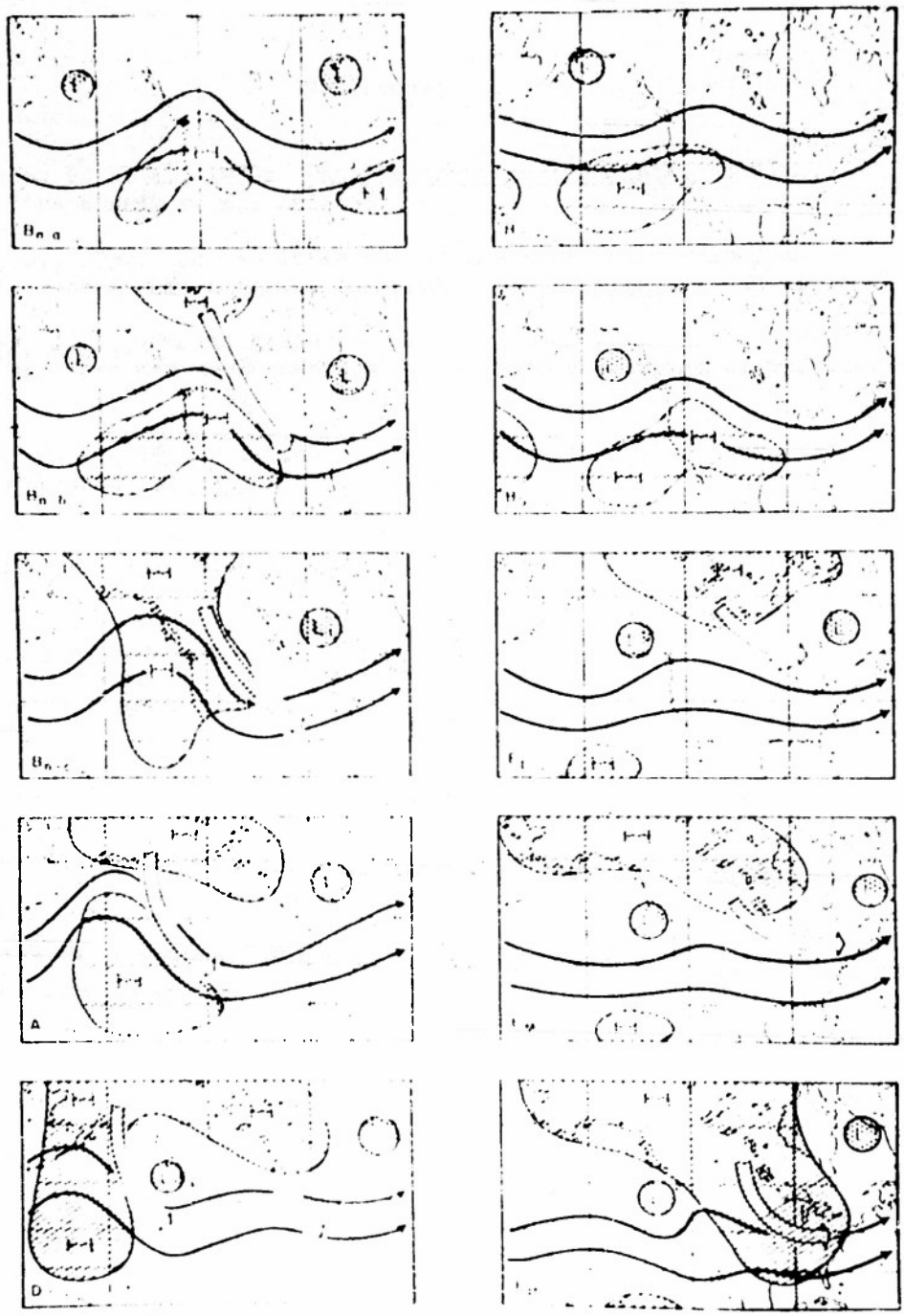

Fig. 10 Schematic diagrams of weather type, where heavy lines with arrows at ends indicate upper-level mean flow, hatched areas are regions of persistent subtropical or polar high pressure at the surface, stippled areas are quasi-stationary low-pressure centers and open-arrows indicate the paths of polar outbreaks.
Left hand: meridional flow type,
Right hand: zonal flow type.

References

1. Bjerknes, V. et al, 1933: Physikalische hydrodynamik. Berlin, Julius Springer, pp. 491-493.

2. Bolin, B., 1950: On the influence of the earth's orography on the general character of the westerlies. Tellus, 2, 184-195.

3. Charney, J. G., and A. Elliassen, 1949: A numerical method for predicting the perturbations of the middle latitude westerlies. Tellus, I(2), 38-54.

4. Eliott, R. D., 1951: Extended-range forecasting by weather type. Compendium meteor., Boston, Amer. Meteor. Soc., 834-840.

5. Hess, S. L., and H. Wagner, 1948: Atmospheric waves in the northwestern United States. J. Meteor., 5, 1-19.

6. Holmboe, J. et al, 1945: Dynamic meteorology. New York, John Wiley and Sons, pp. 326-328.

7. Long, R. R., 1952: The flow of a liquid past a barrier in a rotating spherical shell. J. Meteor., 9, 187-199.

8. Milne-Thompson, L. M., 1950: Theoretical hydrodynamics. New York, Macmillan, pp. 157-160.

9. Oi, M., 1952: Air current crossing a mountain range. J. Meteor. Soc. Jap., 30, 183-189

10. Streeter, V. L., 1948: Fluid dynamics. New York, McGraw-Hill, pp. 116-119 and pp. 112-114.

DATE: MAY 10, 1954

CONTRACT NO. _____
NR NO. _____

DISTRIBUTION LIST FOR UNCLASSIFIED TECHNICAL REPORTS

Addressee	No. of Copies
Geophysics Branch, Code 416, Office of Naval Research, Washington 25, D.C.	2
Director, Naval Research Laboratory, Attention: Technical Information Officer, Washington 25, D.C.	6
Office of Naval Research Contract Administrator, Southeastern Area, c/o George Washington University, 2110 G Street, N.W., Washington 7, D.C.	1
Office of Technical Services, Department of Commerce, Washington 25, D.C.	1
Armed Services Technical Information Center, Documents Service Center, Knott Building, Dayton 2, Ohio	5
Assistant Secretary of Defense for Research and Development, Attention: Committee on Geophysics and Geography, Pentagon Building, Washington 25, D.C.	1
Department of Aerology, U. S. Naval Post Graduate School, Monterey, California	1
Aerology Branch, Bureau of Aeronautics (Ma-5), Navy Department, Washington 25, D. C.	1
Mechanics Division, Naval Research Laboratory Anacostia Station, Washington 20, D. C. Attention: J. E. Dinger, Code 3820	1
Radio Division I, Code 3420, Naval Research Laboratory Anacostia Station, Washington 20, D. C.	1
Meteorology Section, Navy Electronics Laboratory, San Diego 52, California, Attention: L. J. Anderson	1
Library, Naval Ordnance Laboratory, White Oak, Silver Spring 19, Maryland	1
Bureau of Ships, Navy Department, Washington 25, D. C. Attention: Code 327, (Technical Library)	2
Chief of Naval Operations, Navy Department, Washington 25, D. C., Attention: Op-533D	2

Oceanographic Division, U. S. Navy Hydrographic Office, Suitland, Maryland	2
Library, Naval Ordance Test Station, Inyokern, China Lake, California	1
Project Arowa, U. S. Naval Air Station, Building R-48, Norfolk, Virginia	2
The Chief, Armed Forces Special Weapons Project, P. O. Box 2610, Washington, D. C.	1
Office of the Chief Signal Officer, Engineering and Technical Service, Washington 25, D. C. Attention: SIGGGM	1
Meteorological Branch, Evans Signal Laboratory Belmar, New Jersey	1
Office of the Quartermaster General, 2nd and T Sts., Washington 25, D. C., Attention: Environmental Protection Section	1
Office of the Chief, Chemical Corps, Research and Engineering Division, Research Branch, Army Chemical Center, Maryland	2
Commanding Officer, Air Force Cambridge Research Center, 230 Albany Street, Cambridge, Massachusetts, Attention: ERHS-1	1
Headquarters, Air Weather Service, Andrews A. F. Base Washington 20, D. C., Attention: Director Scientific Services	2
Commanding General, Air Material Command, Wright Field, Dayton, Ohio, Attention: MCRESO	1
Commanding General, Air Force Cambridge Research Center, 230 Albany Street, Cambridge, Massachusetts, Attention: CRHSL	1
Commanding General, Air Research and Development Command, P. O. Box 1395, Baltimore 3, Maryland Attention: RDDG	1
Department of Meteorology, Massachusetts Institute of Technology, Cambridge, Massachusetts	1
Department of Meteorology, University of Chicago, Chicago, 37, Illinois	1
Institute for Advanced Study, Princeton, New Jersey	1
The Johns Hopkins University, Department of Civil Engineering, Baltimore, Maryland	1

Scripps Institute of Oceanography, La Jolla, California	1
General Electric Research Laboratory, Schenectady, N. Y., Attention: I. Langmuir	1
St. Louis University, 3621 Olive Street, St. Louis 8, Missouri	1
Department of Meteorology, University of California at Los Angeles, Los Angeles, California	1
Department of Engineering, University of California at Los Angeles, Los Angeles, California	1
Department of Meteorology, Florida State University Tallahassee, Florida	1
Woods Hole Oceanographic Institution, Woods Hole, Mass.	1
The Johns Hopkins University, Department of Physics, Homewood Campus, Baltimore, Maryland	1
New Mexico Institute of Mining and Technology, Research and Development Division, Cocorro, New Mexico	1
Geophysical Institute, University of Alaska, College, Alaska, Attention: C. T. Elvey	1
Blue Hill Meteorological Observatory, Harvard University, Milton 86, Massachusetts, Attention: C. Brooks	1
Department of Meteorology, New York University, New York 53,N.Y.	1
Texas AandM Department of Oceanography, College Station, Texas	1
Rutgers University, College of Agriculture, Department of Meteorology, New Brunswick, New Jersey	1
National Advisory Committee of Aeronautics, 1500 New Hampshire Avenue, NW, Washington 25, D. C.	2
U. S. Weather Bureau, 24th and M Sts., N.W., Washington 25, D. C., Attention: Scientific Services Division	2
Air Coordinating Committee, Subcommittee on Aviation Meteorology, Room 2D889-A, The Pentagon, Washington 25, D. C.	1
American Meteorological Society, 3 Joy Street, Boston 8, Massachusetts, Attention: The Executive Secretary	1
University of Pennsylvania, Department of Meteorology, Philadelphia, Pennsylvania	1
Director of Research, Munitalp Foundation, Inc., 36th Floor, 570 Lexington Avenue, New York 22, New York	1